

## Dynamics of Drop Impact Against Surfaces Covered with Langmuir-Blodgett Layers

Natália Gonçalves,<sup>a</sup> Paulo B. Miranda<sup>b</sup> and Edvaldo Sabadini<sup>\*a</sup>

<sup>a</sup>Departamento de Físico-Química, Instituto de Química, Universidade Estadual de Campinas (UNICAMP), 13083-970 Campinas-SP, Brazil

<sup>b</sup>Instituto de Física de São Carlos, Universidade de São Paulo, P.O. Box 369, 13560-970 São Carlos-SP, Brazil

The dynamics of successive impacts of water droplets against flat glass surfaces covered by Langmuir-Blodgett films of zinc stearate with 1, 3, 5 and 7 layers was investigated. The structure and resistance of monolayers to the impact was evaluated by using fast images of the drop deformation, Brewster angle microscopy (BAM) and contact angle measurements. Eventual disruption (erosion) of the layers was investigated by using sum-frequency vibrational spectroscopy (SFG).

**Keywords:** erosion of monolayers, sum-frequency vibrational spectroscopy, wettability

### Introduction

The impact of droplets on solid surfaces has been widely studied due to the numerous interests of application, such as the study of erosion by rain drops, by inkjet printing, spray cooling on hot surfaces, pesticides application on crops, etc.<sup>1</sup> In this specific case, the study of drop impact of solutions of pesticides against the surface is important due to the fact that many leaves have high hydrophobicity. Therefore, a significant portion of the agrochemical solution tends to be ejected from the leaf and fall to the ground.<sup>2</sup>

Due to advances in technologies for high speed photography, drop-surface impact investigations have been highly improved over the years. When colliding against a surface, the droplet undergoes a sequence of deformations in the range of milliseconds, changing the total solid-liquid interface energy in this short time interval. This energy is totally related to the physico-chemical characteristics of the drop and the surface.

There are several known super hydrophobic surfaces in nature. In 1997, Barthlott and Neinhuis<sup>3</sup> related for the first time the super hydrophobicity and self-cleaning property of a lotus leaf (*Nelumbo nucifera*) to its rough and waxy surface. Since then, several studies have been conducted in order to reproduce synthetic surfaces with similar properties.

In order to mimetize the natural structures, several techniques have been used to produce super hydrophobic surfaces. The main ones are: lithography,<sup>4</sup> template,<sup>5</sup>

electrospinning,<sup>6</sup> sol-gel,<sup>7</sup> electrochemical deposition,<sup>8</sup> deposition by chemical evaporation (CVD),<sup>9</sup> Langmuir-Blodgett,<sup>10-12</sup> among others.

The Langmuir-Blodgett technique is a simple method to produce thin organic films on substrates and allows, beyond the control of film thickness, a high degree of molecular organization.<sup>13</sup> It is very difficult to obtain this high level of control over the orientation and arrangement of the molecules in the formation of layers by other deposition methods.

The dynamics of droplet impact against solid surfaces has been widely studied, and driven by many industrial and fundamental interests.<sup>14</sup> From a fundamental point of view, the wealth of concepts that need to be considered in the approach to this process is immense, from rheology to interface chemistry. The result of the impact of falling droplets depends on several factors such as the impact speed, the direction onto the surface, the droplet size, liquid properties (density, viscosity, viscoelasticity and some other non-Newtonian effects for rheologically complex fluids) and the surface tension.<sup>15</sup> Furthermore, the study of the impact of drops on solid surfaces is complex, because besides the aforementioned factors, one should also consider the nature of the surface of impact, such as wettability and roughness.<sup>16,17</sup>

When impinging against the surface, the droplet undergoes a sequence of deformations in the range of milliseconds, changing, in this brief interval, the energy of the solid-liquid interface of the system<sup>15</sup> and, depending on their kinetic energy, surface hydrophobicity, and chemical

\*e-mail: sabadini@iqm.unicamp.br

nature of the liquid, part of the droplet can be ejected after rebound.

The present investigation aimed at studying the impact of water droplets against hydrophobic surfaces. These surfaces were obtained by monolayer deposition of zinc stearate on glass using the Langmuir-Blodgett technique (LB). The main goal was to evaluate how the chemical nature of the solid surface may influence the drop deformation after impact, as well as evaluating the resistance of the monolayers to eventual erosion. The latter was evaluated by the drop deformation, liquid-solid contact angle and sum-frequency spectroscopy (SFG), before and after consecutive impacts. The uniformity of the films before impact was investigated by Brewster angle microscopy (BAM).

## Experimental

### Substrate pre treatment

The solid supports used in this experiment for deposition of monolayers were glass slides. First of all, substrates were cleaned with chloroform in order to remove possible fats present on their surface. Then, they were dipped in ethyl alcohol in a ultrasonic bath for 5 min. The plates were transferred to a beaker containing distilled water, and remained immersed until use.

### Chemicals and solutions

All solvents and reagents were used without further purification.

Solution of stearic acid (octadecanoic acid, Aldrich, 99% purity) was prepared in chloroform at a concentration of  $1.0 \text{ mmol L}^{-1}$ . Aqueous subphase for the LB-transfer was prepared by dissolving  $0.1 \text{ mmol L}^{-1}$  of zinc acetate (Aldrich, 99.99% purity) in ultrapure water (Millipore, resistivity  $18.2 \text{ M}\Omega \text{ cm}$ ).

### Langmuir-Blodgett (LB) films

The isotherms and LB deposition were carried out using a computer-controlled trough from INSIGHT with a surface area of  $459 \text{ cm}^2$ . Prior to the experiment, the trough was rigorously cleaned with pure water and chloroform. The trough was then filled with the subphase and thermostated at  $20 \text{ }^\circ\text{C}$ . Subsequently,  $150 \mu\text{L}$  of stearic acid (SA) solution was spread onto the subphase to form an interfacial film. Around 5 min are allowed in order to the solvent be evaporated and the SA layer to spread before initiating the compression and transfer. The SA monolayers

were compressed to a surface pressure of  $30 \text{ mN m}^{-1}$  and transferred to the substrate by vertical dipping method with a deposition rate of  $0.042 \text{ mm s}^{-1}$ . A drying time of 10 min was used after each lift/dip.

### Fast imaging of drop impact and image treatment

The images of the droplet impact on the surfaces were obtained using the experimental apparatus shown schematically in Figure 1.

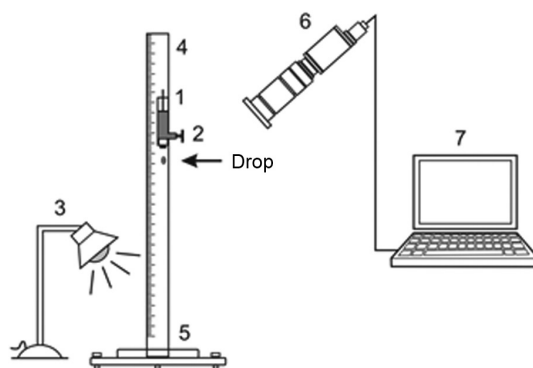


**Figure 1.** Scheme of the experimental apparatus used to generate the drops and image acquisition: (1) fluid reservoir tube (burette); (2) valve to release drop; (3) lighting system; (4) ruler; (5) impact base; (6) camera and (7) computer.

The valve is opened and the droplet is formed slowly, detaching from the burette spontaneously. The droplet falls from a height of 60 cm and collides with the surface. A LED light (blue) system was used for illumination.

Three consecutive shocks were filmed in the same spot of the flat glass. After each impact, the droplet was carefully removed from the surface with a tissue by capillarity, taking due care so that it does not touch the glass surface.

All tests were performed in duplicate with two different plates prepared under the same experimental conditions. The images were obtained using a digital high-speed camera (Photron 1024PCI CMOS model 100KC), coupled with an objective lens Nikon zoom ( $1\times$ ). The images were obtained at  $6000 \text{ frames s}^{-1}$ .

The images were processed using Image J software (MacBiophotonics, <http://www.macbiophotonics.ca/downloads.htm>). The contact areas (solid-liquid) between the droplet and the surface were determined at different time intervals during expansion and contraction of the droplet on the surface.

### Contact angle

The determination of the contact angle between the water droplet and the different surfaces was performed

using an optical tensiometer (Theta, Science Biolin). The contact angles (at the equilibrium) of water droplets (15  $\mu\text{L}$ ) on cover slips with different numbers of monolayers were obtained before and after the three impacts.

### SFG spectroscopy

A commercial SFG spectrometer (Ekspla, Lithuania) was used for the nonlinear vibrational spectroscopy measurements. Its source is a  $\text{Nd}^{3+}$ :YAG laser (1064 nm) with 30 ps pulses of ca. 30 mJ and 20 Hz repetition rate. For sample excitation, the wavelength in the visible region was 532 nm (corresponding the 2<sup>nd</sup> Harmonic of the laser) with an average energy of 900  $\mu\text{J}$  and 60° incidence angle, and an infrared beam tunable in the range 1000-4000  $\text{cm}^{-1}$  with an average pulse energy between 30 and 150  $\mu\text{J}$ , and incidence angle 51°. The polarizations of the beams used were SFG (s); Vis (s); IR (p). The overlap area of the visible and IR beams on the sample was about 1  $\text{mm}^2$ . The spectral region of interest in this work was the CH stretching (2800 to 3000  $\text{cm}^{-1}$ ), which was scanned at intervals of 3  $\text{cm}^{-1}$  with each data point being an average of 100 laser shots. The spectral resolution of the IR pulse generated by the optical parametric amplifier and difference frequency generation stage was 3  $\text{cm}^{-1}$ . The SFG measurements were obtained before and after three impacts, at the same point in the glass covered with monolayers.

### Brewster angle microscopy (BAM)

A commercial BAM microscope (Nanofilm GmbH) was used for imaging the transferred monolayers and assessing their homogeneity.

## Results and Discussion

A sequence of photographs obtained after the impact of a drop against the bare surface of glass and covered with a certain odd number of monolayers ( $n$ ) are shown in Figure 2 and a film of a drop impact can be seen in the Supplementary Information (SI) section.

The spreading of the drops takes approximately 4 ms and no important variations on the morphology of the droplet area are observed for the surfaces. However, the retraction of spread liquid is sensitive to the coverage. At the end of the process, a shallow film remains spread at the surfaces for  $n = 0$  and 1, indicating certain wettability. When  $n > 1$ , the rim of the disk is more fragmented for surfaces covered with more than three layers, in comparison with the disk of liquid retracting on the glass surface.

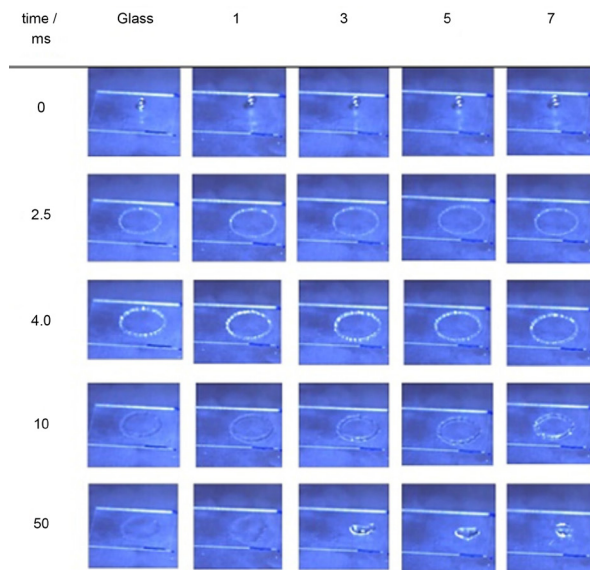


**Figure 2.** Sequence of photos obtained after the impact of droplets against glass surface and on glass surface covered with 1, 3, 5, and 7 monolayers. At the left are indicated the times (in ms) after the first contact of the drop with the surface in which the photos were taken.

The result obtained with the surface covered by a single layer ( $n = 1$ ), has motivated to understand if the wettability was consequence of irregular coverage or it is related to the fragility of the monolayer. The impact could cause erosion of the monolayer, partially exposing the drop of water to the glass surface. In order to investigate the capability of the monolayers to resist against eventual erosion caused by the drop impact, sequences of impacts over the same area were filmed. For better analysis of the temporal development of the film diameter spread on the surface, some considerations must be made. It is common in the literature (see references 18 and 19) to express the dynamics in dimensionless parameters. Therefore, the time is converted to  $t^* = tV/D$  ( $t$  = time,  $V$  = the initial impact velocity of the drop,  $D$  = the initial drop diameter). In order to use a dimensionless diameter, the spreading factor is used, which is defined by  $d^* = d/D$  ( $d$  = diameter of the contact area of the liquid on the surface,  $D$  = the diameter of the droplet before impact).<sup>2,18,19</sup> These transformations are essential when comparing the behavior of droplets of different liquids impacting on several solid surfaces. In this paper, only impacts of water droplets were studied, but these considerations are still necessary in order to avoid possible variations in size of droplets formed in each impact and camera positioning during the filming. Furthermore, this processing provides better visualization of the results in comparison with previously data reported in the literature.

The dependence of the expansion factor,  $d^*$ , of the liquid in different times (normalized) for the surfaces is plotted in Figure 3.

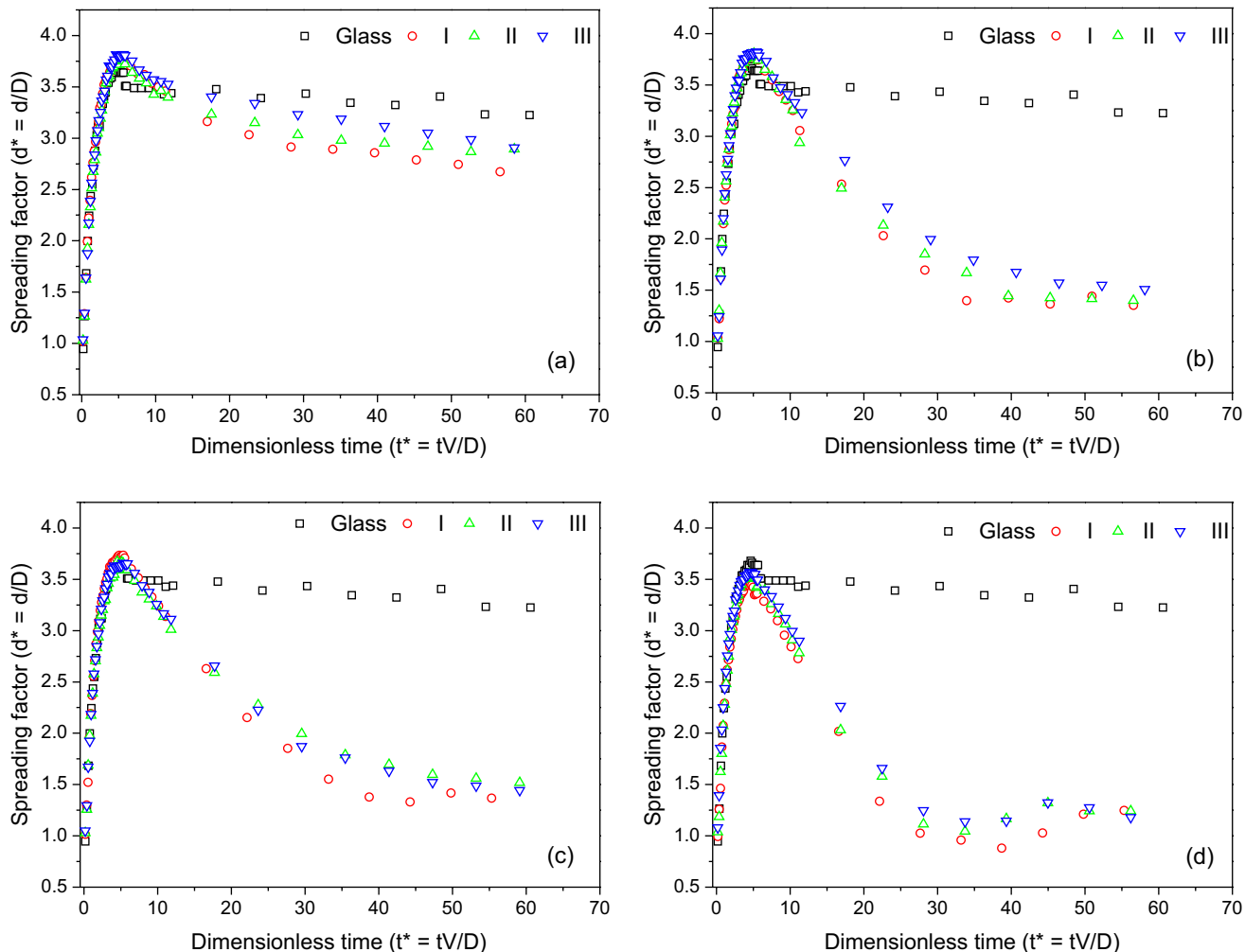


**Figure 3.** Dependence of the expansion factor as a function of time for a sequence of three impacts (I, II and III) on surfaces covered with: 1 (a); 3 (b); 5 (c) and 7 (d) monolayers. The result for the impact against the bare-glass surface is also indicated as a reference.

The reproducibility of the whole process was investigated by filming the drop impact in two independent experiments. The impacts of two drops against two surfaces with the same number of layers were filmed. During the expansion process, the variation of the expansion factor is lower than 5% but larger differences (35%) were observed during the drop retraction.

Except for the surface with  $n = 1$ , the results for the consecutive impacts over the other covered surfaces revealed that the spreading-contraction processes are not significantly affected by the sequence of drops. This means that under such experimental conditions, the layers are apparently resistant to disruption by drop impact. Conversely, the damage may result in the removal of a bilayer, maintaining the same wettability overall.

Therefore, the increased wettability for the single layer film ( $n = 1$ ) suggests that the monolayer transfer to the glass surface is not complete. We have confirmed this by taking images of the films with BAM. An example is shown in

Figure 4, but all films have shown the presence of partial coverage, with regions of different film thicknesses.

This explains why the single layer film presents larger wettability and susceptibility to damage by drop impact, while the other films with  $n > 1$  are more hydrophobic and resistant to damage. The many layers eventually cover all the glass surface, presenting only hydrophobic alkyl chains exposed to air, and eventual damage possibly remove only the additional layers that are weakly bonded to the first one.

The contact angles of sessile drops of water positioned on the regions of the impacts were determined, in order to verify changes of the wettability caused by destruction of the monolayers (Figure 5).

The values for contact angles obtained for the surfaces are shown in Table 1.

The results of the contact angle are in agreement with the observations of the spreading-contraction process observed in the films. The surface covered with only one monolayer is indeed more wetted in comparison with the

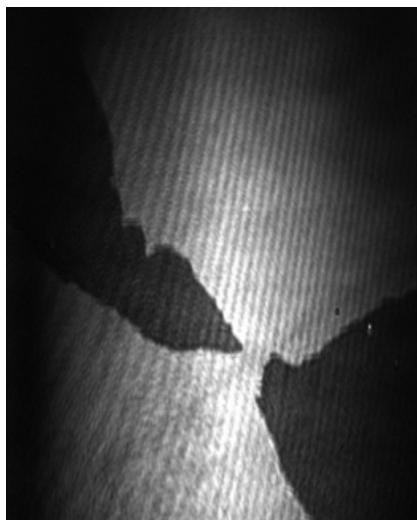


**Figure 4.** BAM image of a 3-layer LB film of zinc stearate on glass, before drop impact. The image size is 300 (H)  $\times$  375 (V)  $\mu\text{m}^2$ . Brighter regions correspond to thicker films. The nearly vertical pattern of fine lines is an artifact due to interference of the laser reflection on the back side of the substrate.

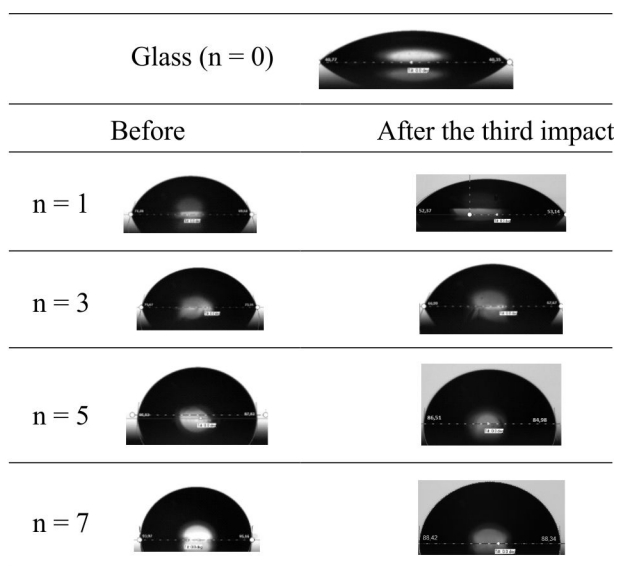


**Figure 5.** Pictures of sessile drops on surfaces of glass, and over surfaces covered with 1, 3, 5 and 7 monolayers, before and after the impact of three drops.

**Table 1.** Values for the contact angle ( $^\circ$ ) for water on glass and on surfaces covered with  $n$  layers of Zn Stearate without impact and after the impact of three drops

Number of layers ( $n$ )	Without impact	After three impacts
Glass (0)	$44 \pm 4$	–
1	$70 \pm 3$	$57 \pm 5$
3	$76 \pm 2$	$66 \pm 2$
5	$86 \pm 2$	$85 \pm 1$
7	$93 \pm 2$	$88 \pm 1$

surfaces containing more layers. The values for the contact angle increases with the number of layers, indicating a progressive hydrophobicity. This can be associated with certain inhomogeneity of the layers, as seen in the BAM images (Figure 4). The transfer rates (TR) observed during the depositions were: 0.5–0.7 and 0.9–1.1 for even and odd numbers of monolayers, respectively. Although we have used in our experiments only films with odd numbers of layers (that are hydrophobic), during their fabrication the even layers, being less perfect, do affect the quality of the final odd-layered film. According to the results, the contact angle of the surfaces covered with 1 and 3 layers change to lower values of contact angle after 3 drop impacts, but negligible variation is observed for 5 and 7 layers.

The inhomogeneity during the preparation of the monolayers and eventual modification caused by drop impact were investigated by using Sum-frequency generation vibrational spectroscopy (SFG spectroscopy). This (non-linear) vibrational spectroscopy is appropriate to investigate molecular orientation at interfaces, as only the spectrum of a non-centrosymmetric media is obtained.<sup>20,21</sup> Therefore, based on this condition, the homogeneity of lipid layers on a glass plate can be investigated. In Table 2 are indicated the vibrational modes for  $\text{CH}_2$  and the terminal  $\text{CH}_3$  groups of alkyl chains and their correspondent wavenumbers.

**Table 2.** Wavenumbers and correspondent stretching modes for the CH groups of alkyl chains observed by SFG<sup>21</sup>

Mode	Frequency / $\text{cm}^{-1}$
Symmetric stretching of $\text{CH}_3$	ca. 2878
Fermi resonance of $\text{CH}_3$	ca. 2940
Anti-symmetric stretching of $\text{CH}_3$	ca. 2965
Symmetric stretching of $\text{CH}_2$	ca. 2848
Anti-symmetric stretching of $\text{CH}_2$	ca. 2915

For a surface perfectly covered with a densely packed monolayer (for which  $\text{TR} = 1$ ) the peaks associated with the stretching of the terminal  $-\text{CH}_3$  group dominates the spectrum, because the modes of the  $\text{CH}_2$  groups along the chain are inactive due to their centrosymmetrical arrangement.<sup>22</sup> For an even number of densely packed Zn stearate layers (not used in this work), they form a centrosymmetrical arrangement and no SFG spectrum is detected. Therefore, in the ideal case of perfectly transferred layers, the films with even number of layers would show vanishing SFG signals and those with odd numbers should all yield the same spectrum, dominated by contributions from the terminal  $\text{CH}_3$  group of the last layer.<sup>23,24</sup> However, if a layer is not densely packed, the alkyl chains present *gauche* conformations that break the inversion symmetry of

the CH<sub>2</sub> groups along the chain, so that the SFG spectrum has now contributions from both CH<sub>2</sub> and CH<sub>3</sub> groups. Hence, the intensity ratio for the CH<sub>2</sub> and CH<sub>3</sub> symmetric stretches is a qualitative indicator of the conformational order of the monolayers.<sup>22,25</sup>

Figure 6 shows the SFG spectra for the plates covered with the Zn stearate layers before the drop impact. The peaks associated with the vibrational modes listed in Table 2 are indicated. According to the spectra of Figure 6a (and Figure 6b), the intensity of the peaks increases with the number of layers. The SFG intensity for the 7-layer film is nearly the same for a perfect LB monolayer. As previously mentioned, this trend would not be expected for perfectly ordered layers, and therefore is associated with some inhomogeneity produced during the transfer of the monolayers to the plate, probably more pronounced for the even numbers, as indicated by their lower transfer ratio and the BAM images (see Figure 4).

The SFG spectra for the surfaces covered with one and seven layers, before and after the impact of three droplets,

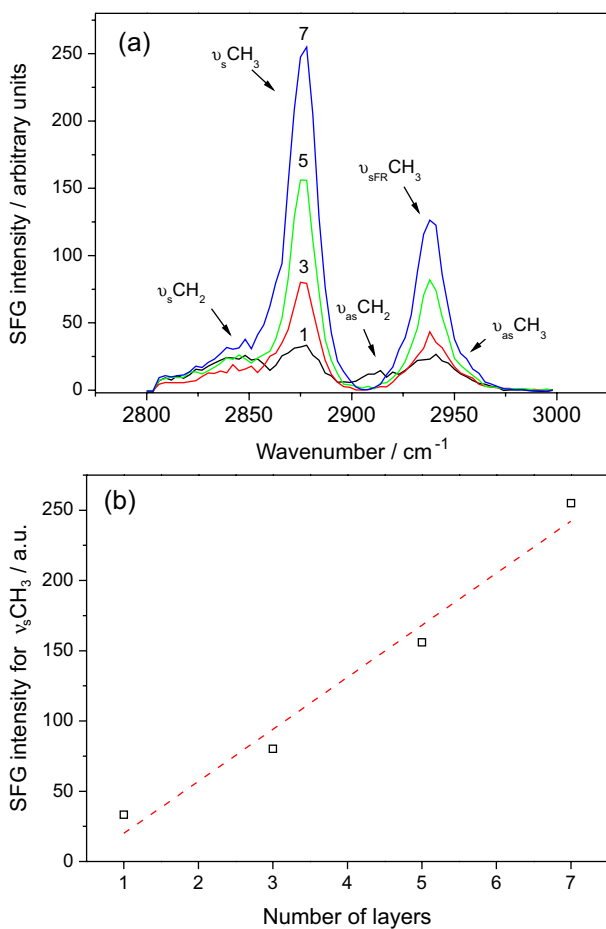


**Figure 6.** (a) SFG spectra for the glass surface covered with several Zn stearate layers (the attributions of the correspondent stretching modes are indicated according to Table 2); (b) intensity of the peak associated with the symmetric stretching of CH<sub>3</sub> as a function of the number of layers.

are shown in Figure 7. Contrary to the surface covered with only one layer (Figure 7a), negligible variations are observed in the spectra for the seven-layer film (Figure 7b) after the impact of the drops.

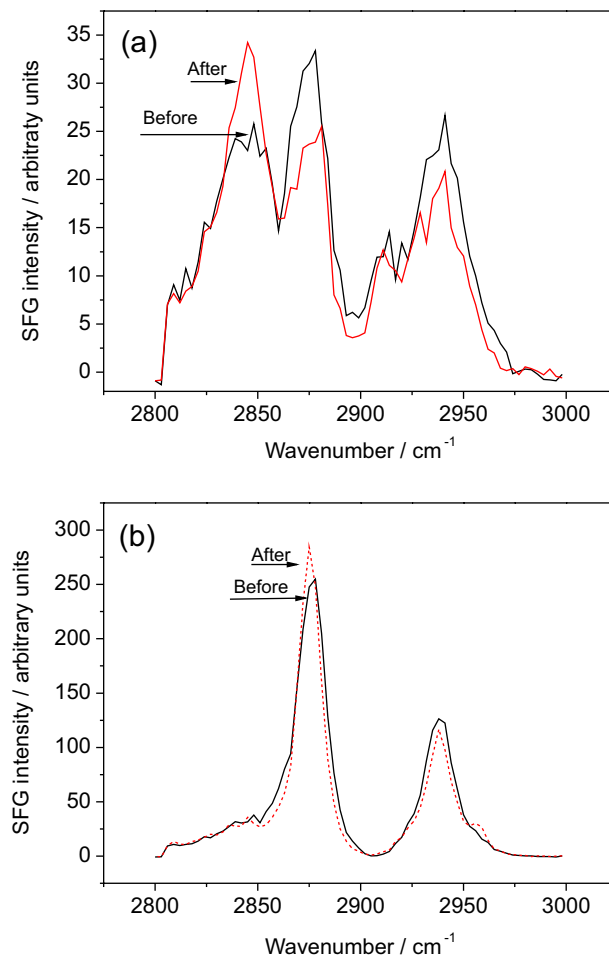


**Figure 7.** SFG spectra for the surfaces covered with (a) one and (b) seven layers, before and after the impact of three droplets.

For the seven layers, the SFG spectra indicate they are nearly perfect densely packed before and after the impacts. We infer that in this case, the interactions between the molecules of stearate preserve the integrity of the monolayer under such impact conditions. However, a small decrease of the CH<sub>3</sub> symmetric stretch (2878 cm<sup>-1</sup>) and increase of the CH<sub>2</sub> symmetric stretch (2848 cm<sup>-1</sup>) are observed for the one-layer film. This indicates that films already with partial coverage and *gauche* defects have the conformational disordered of the alkyl chains increased, possibly due to the erosion caused by the drop impact.

## Conclusions

The fast images of the droplet deformation obtained after their impact against surfaces covered with LB layers

of Zn stearate revealed that their spreading mechanism is independent of the nature of the surface. However, the retraction is sensitive to variations on the nature of the surface. For the impact on surfaces covered with only one LB monolayer of partial coverage, the surface is more wettable in comparison with surfaces covered with more layers. Under the experimental drop impact conditions, the LB monolayers revealed to be very resistant to the eventual erosion caused by sequence of drop impacts, except for the more wettable one-layer film. The results based on the fast images of the drop deformation, are supported by measurements of SFG spectroscopy, in which the integrity of the external layer is evidenced.

## Supplementary Information

A film of a drop impact against a glass surface covered with Langmuir-Blodgett monolayers of zinc stearate can be seen in Supplementary File available free of charge at <http://jbc.ssbq.org.br> as wmv file.

## Acknowledgments

The authors thank the Brazilian agencies CNPq, and Fapesp for financial support and fellowship. We also thank Professor Maria Elisabete D. Zaniquelli for the preparation of the LB substrates, Thais Cristina Destefani for the experiments of drop impact used in the picture of the Graphical Abstract and Iveraldo Rodrigues for his help with the pictures.

## References

- Scheller, B. L.; Bousfield, D. W.; *AIChE J.* **1995**, *41*, 1357.
- Wirth, W.; Storp, S.; Jacobsen, W.; *Pestic. Sci.* **1991**, *33*, 411.
- Barthlott, W.; Neinhuis, C.; *Planta* **1997**, *202*, 1.
- Zhang, X.; Zhao, J.; Zhu, Q.; Chen, N.; Zhang, M.; Pan, Q.; *ACS Appl. Mater. Interfaces* **2011**, *3*, 2630.
- Abdelsalam, M. E.; Bartlett, P. N.; Kelf, T.; Baumberg, J.; *Langmuir* **2005**, *21*, 1753.
- Muthiah, P.; Hsu, S. H.; Sigmund, W.; *Langmuir* **2010**, *26*, 12483.
- Manca, M.; Cannavale, A.; De Marco, L.; Arico, S. A.; Cingolani, R.; Gigli, G.; *Langmuir* **2009**, *25*, 6357.
- Darmanin, T.; Guittard, F.; *J. Am. Chem. Soc.* **2009**, *131*, 7928.
- Meng, L. Y.; Park, S. J.; *Mater. Chem. Phys.* **2012**, *132*, 324.
- Roberts, G. G.; *Langmuir Blodgett Films*; Plenum Press: New York, 1990.
- Puggelli, M.; Gabrielle, G.; Caminati, G.; *Thin Solid Films* **1994**, *244*, 1050.
- Gabrielle, G.; Puggelli, M.; Ferroni, E.; Carubia, G.; Pedrocchi, L.; *Colloids Surf.* **1989**, *41*, 1.
- Uzunoglu, T.; Çapan, R.; Sari, H.; *Mat. Chem. Phys.* **2009**, *117*, 281.
- Klein, J.; *Nature* **2000**, *405*, 745.
- Frohn, A.; Roth, N.; *Dynamics of Droplets*, Springer-Verlag: Berlin, 2000.
- Yarin, A. L.; *Annu. Rev. Fluid Mech.* **2006**, *38*, 159.
- Tsai, P.; Pacheco, S.; *Langmuir* **2009**, *20*, 12293.
- Rioboo, R.; Marengo, M.; Tropea, C.; *Exp. Fluids* **2002**, *33*, 112.
- Sikalo, S.; Ganié, E. N.; *Exp. Therm. Fluid Sci.* **2006**, *31*, 97.
- Shen, Y. R.; *PNAS* **1996**, *93*, 12104.
- Lambert, A. G.; Davies, P. B.; Neivandt, D. J.; *Appl. Spectrosc. Rev.* **2005**, *40*, 103.
- Guyot-Sionnest, P.; Hunt, J. H.; Shen, Y. R.; *Phys. Rev. Lett.* **1987**, *59*, 1597.
- Nishida, T.; Johnson, C. M.; Holman, J.; Osawa, M.; Davies, P. B.; Ye, S.; *Phys. Rev. Lett.* **2006**, *96*, 077402.
- Silva, H. S.; Miranda, P. B.; *J. Phys. Chem. B* **2009**, *113*, 7491.
- Keszthelyi, T.; Holló, G.; Nyitrai, G.; Kardos, J.; Héja, L.; *Langmuir* **2015**, *31*, 7815.

Submitted: August 12, 2015

Published online: September 22, 2015

FAPESP has sponsored the publication of this article.